Long-lasting intense cut-off lows to become more frequent in the Northern Hemisphere

Article

It is advisable to refer to the publisher's version if you intend to cite from the work. See Guidance on citing.

www.reading.ac.uk/centaur

CentAUR

Central Archive at the University of Reading

Reading's research outputs online

Article

Long-lasting intense cut-off lows to become more frequent in the Northern Hemisphere

Check for updates

Aditya N. Mishra [1] ✉, Douglas Maraun [1], Reinhard Schiemann [2], Kevin Hodges[2], Giuseppe Zappa [3] & Albert Ossó [1]

Cut-off Lows are slow-moving mid-latitude storms that are detached from the main westerly flow and are often harbingers of heavy and persistent rainfall. The assessment of Cut-off Lows in climate models is relatively limited, in fact, there are no studies conducted on the future changes of Cut-off Lows within climate models. Given the importance of Cut-off Lows in leading to severe hazards, here we study them in Coupled Model Intercomparison Project Phase 6's worst-case future simulations (SSP5-8.5). Most (80%) of the models show that Cut-off Lows with high intensity and longer lifetimes are projected to become more frequent in spring over the land regions of the Northern Hemisphere. Such an increase in Cut-off Low frequency could substantially increase related potential hazards. An increase in Cut-off Low propagation velocity, however, may partly offset this increase in hazard. Lastly, projected changes in the jet stream with possible dynamical linkages to Cut-off Lows corroborate the findings of this study.

Cut-off Lows (COLs) are middle- and upper-tropospheric low-pressure systems that are detached from the main westerly flow on the equatorward side[1]. They are generally characterized by a cold core, high potential vorticity (PV) anomalies, and closed geopotential height contours[1]. The detachment of the system from the westerly flow is due to Rossby wave breaking (RWB), and results in COLs maintaining a slower propagation speed compared to frontal systems[2]. Importantly, COLs are often harbingers of sustained precipitation leading to catastrophic extreme rainfall-related impacts such as floods and landslides[3–6]. The heavy precipitation is caused by deep convection[7], which occurs when the cold air associated with the upper-level low destabilizes the air column beneath it, as it interacts with warmer mid-latitude air[8]. A recent calamitous example of this was the European flooding of July 2021 that was caused by a quasi-stationary COL[9] and left over 200 people dead in addition to billions of Euros in damages[10]. Besides producing heavy precipitation, COLs are also responsible for pulling stratospheric ozone down from the lower stratosphere into the upper and middle troposphere[11,12]. Once in the troposphere, ozone acts as a diverse pollutant with the potential to negatively impact human health, agricultural crop yields, and also function as a greenhouse gas[13].

COLs have long been the subject of thorough studies that have examined their physics[1] and climatology across both hemispheres[14,15]. The genesis of COLs is associated with the rapid and irreversible deformation of potential vorticity contours (RWB)[2], that allows the excursion of high potential vorticity stratospheric air southwards into the troposphere[16]. This aids in inducing higher cyclogenetic forcing in the air column that is fundamental to the convection associated with COLs[17]. COLs follow a typical lifecycle whereby most of their energy is imported through ageostrophic flux convergence and other baroclinic processes associated with the parent jet stream[18]. They decay due to diabatic heating and friction[8], unless there is an injection of new air into the cutoff low with high potential vorticity.

In recent years, considerable improvements have been made in observation data quality and computational capabilities. These advances have motivated enhanced research on COLs using available observations[19–21], historical modeled data[22], as well as in event attribution studies[23]. The representation of COLs in historical simulations of the Coupled Model Intercomparison Project, Phase 6 (CMIP6) exhibits an all-around improvement compared to its predecessor, CMIP5[22]. This improvement is particularly true for the frequency and maximum intensity (vorticity) distribution of COLs, offering a crucial advantage as the latter is directly correlated with accumulated precipitation[24]. These recent findings have not only broadened our understanding of COLs but have also established the foundation for assessing the associated impacts in climate attribution studies that are not limited to single events. However, a similar but all the more important assessment of future changes in impacts due to climate

¹Wegener Center for Climate and Global Research, University of Graz, Graz, Austria. ²National Centre for Atmospheric Science, Department of Meteorology, University of Reading, Reading, UK. ³Institute of Atmospheric Sciences and Climate, Italian National Research Council, Bologna, Italy. ✉e-mail: aditya.mishra@geo.uu.se

change is not possible, as there is currently no information on changes in COL projections in the future.

This study precisely fills this gap with a multi-model (CMIP6) analysis of the projected changes in COLs in the Northern Hemisphere. The analysis focuses on the key characteristics that determine the impact of a COL - frequency, duration, intensity, and propagation velocity[20,25–27]. To assess the influence of climate change on these characteristics, the following questions have been formulated:

1. How will climate change impact the frequency of COLs in the Northern Hemisphere?
2. How are the most intense and long-lasting COLs affected by climate change?
3. How will the propagation velocity of COLs change with climate change?

To detect and trace COLs, recent studies have mainly used three different approaches: the conceptual model-based on Geopotential Height, the PV-based detection scheme, and the relative vorticity-based TRACK algorithm. While the conceptual cut-off low model assumes a cold core at the cut-off low center, a thickness ridge, and a baroclinic zone ahead of the low[14], the potential vorticity framework is a contour searching algorithm used to identify the dynamical tropopause[8,28]. The climatologies from these two approaches are spatially comparable, however, there are uncertainties due to a missing consensus on some of the core features regarding the structure of cut-off lows[14,28–30]. In particular, Potential vorticity (PV) structures can vary with altitude across different isentropes[19], so different isentropic levels must be used for PV feature detection, depending on the season and region[31,32]. In the conceptual model, on the other hand, uncertainties arise due to the varying presence and vertical location of the cold core[21].

In this study, TRACK—a widely used feature detection tool, is used as an alternative method for detecting cut-off lows[33–35]. It focuses on robust features such as low pressure at the center and cyclonic circulation, which can be identified at high-pressure levels where these systems develop. A limitation of this approach is its neglect of the cold core's presence; however, this omission also circumvents uncertainties associated with identifying its vertical location. The analysis is conducted for the historical (1950–2014) and the future scenario SSP5-8.5 (2071–2100) runs of 18 CMIP6 models (Supplementary Table 1). The chosen models had zonal/meridional wind data at 250 hPa pressure level, necessary for relative vorticity calculation, available at the time of writing this article. The detected COLs are studied for projected changes in frequency and propagation velocity in the Northern Hemisphere. To distill relevant information on the changes in potential impacts, the focus of the investigation is on long-lasting and high-intensity COLs.

Results

The seasonal climatology of COLs is studied using the European Centre for Medium-Range Forecast's (ECMWF) fifth-generation reanalysis (ERA5) dataset. During winter, COL activity predominantly occurs along the western coast of North America and stretches from the Moroccan coast in Northwestern Africa across the Mediterranean Sea (Fig. 1a). This pattern persists into spring, with notable intensification over the European landmass (Fig. 1b). In the summer, COL activity reaches its overall peak in the northern hemisphere with a dramatic surge over Asia-N. Pacific, alongside a rise over Europe as well as North America (Fig. 1c). In the autumn, sustained COL activity continues along the western North American coast, but a reduction is seen over Europe and Asia-N.Pacific (Fig. 1d).

The ability of the CMIP6 models to reproduce the observed seasonal climatology is evaluated by calculating the absolute bias in the ensemble mean compared to the ERA5 reanalysis. A consistent negative bias is observed across all seasons in regions of major COL activity. This includes the North American west coast, Europe, the Mediterranean Sea, the Western Atlantic, and the Asia-N.Pacific region (Fig. 1e–h). It is essential to acknowledge that certain regions, such as central Asia, experience a much lower frequency of COLs. Consequently, biases in these regions, regardless

of their sign, may have limited relevance for the overall interpretation. Therefore, for the forthcoming analysis, we limit ourselves to regions that have been previously identified by ref. 29 for having high COL activity[14]. Land regions of Europe and North America (Fig. 1a) are also included and would be important for the examination, given their exposure to COL-related hazards.

Projected changes in COL frequency

To study the future changes in COLs, the COLs identified in the CMIP6 SSP5-8.5 projections are compared to those from the historical simulations across the four seasons. This is illustrated using the mean percentage changes in the spatial distribution of COLs (Fig. 1i–l). Since absolute COL numbers vary from region to region, this analysis is complemented with boxplots illustrating the absolute number of COLs in a given region for historical datasets and future (SSP5-8.5) datasets (Fig. 1m).

Overall, a small median increase of 5% in COL frequency is projected over Europe in winter (Fig. 1i, m), transitioning to a more substantial median increase in spring (20%) (Fig. 1j, m). The projected changes over central and northern Europe show a statistically significant increase of up to 50% in some areas (Fig. 1j). In both seasons, 15/18 models show an increase in the future. In summer and autumn, however, the projected changes in COL frequency are minimal owing to uncertainties in the models over the direction of change (Fig. 1k–m). COL frequency in the western Mediterranean Sea and southwestern Atlantic is projected to decline throughout the year (Fig. 1m).

COL frequency over North America is minimal in the winter months (median of 5 COLs/season). In spring, however, the COL frequency is much more, and an overall positive median change of 15% is projected with a northward shift in the pattern along the west coast (Fig. 1j, m). Importantly, 15/18 models show a positive change in COL frequency in spring, with significant positive changes in the northwest of the continent. In summer, however, 14/18 models project a decrease with a negative median change of 5% (Fig. 1k, m). A significant mean positive change (50–70%) is projected for the Mexican west coast in summer (Fig. 1k), offset by negative changes further north (up to 50%) (Fig. 1k). As a result, the frequency changes over the East Pacific remain neutral during the summer months, in contrast to other seasons, where they show a decline (Fig. 1m).

In Asia-N.Pacific, substantial inter-seasonal variability is seen, whereby COL activity in summer is much more frequent than in the other seasons (Fig. 1c, m). Here, a surge in COL activity is projected with climate change in winter, spring, and autumn (Fig. 1i, j, l, m). In all three seasons, more than 80% of the models project a positive change, with a 20% median increase in winter. In the summer, however, there is a projected decline in COL frequency, with 13/18 models showing a decrease (Fig. 1k, m). The overall negative change in summer is owing to a substantial reduction in mean (up to 30%) in the high COL activity region of northeastern Asia-N.Pacific (Fig. 1k). Additionally, in autumn, a strong poleward shift in pattern is projected (Fig. 1i). Noticeably, the ensemble spread is relatively very large in summer and autumn compared to any other season and region (Fig. 1m).

Projected changes in COL frequency: duration and intensity classes

Most COLs last for 2–4 days, while the longest-lasting COLs may go even beyond 10 days of lifetime[14]. However, the duration of COLs may vary slightly depending on the tracking method used[32]. The lifetime (duration) of a COL is a critical characteristic that potentially determines the associated precipitation[27]. Thus it is imperative to study how climate change will influence the frequency of COLs that are long-lasting. To this end, all detected COLs are divided into two classes based on their lifetime (duration) —COLs that last 1–3 days (short-lasting) and COLs that last over 3 days (long-lasting). Moreover, COLs that last long, also tend to achieve a higher intensity maxima in their lifetime[36]. To discretely identify COLs that are more intense, a threshold of $10 \times 10^{-5}\ \mathrm{s^{-1}}$ is chosen, as the median change in accumulated precipitation has been found to surge by 80% around this value[24]. Therefore, the two intensity maxima-based classes are— COLs with
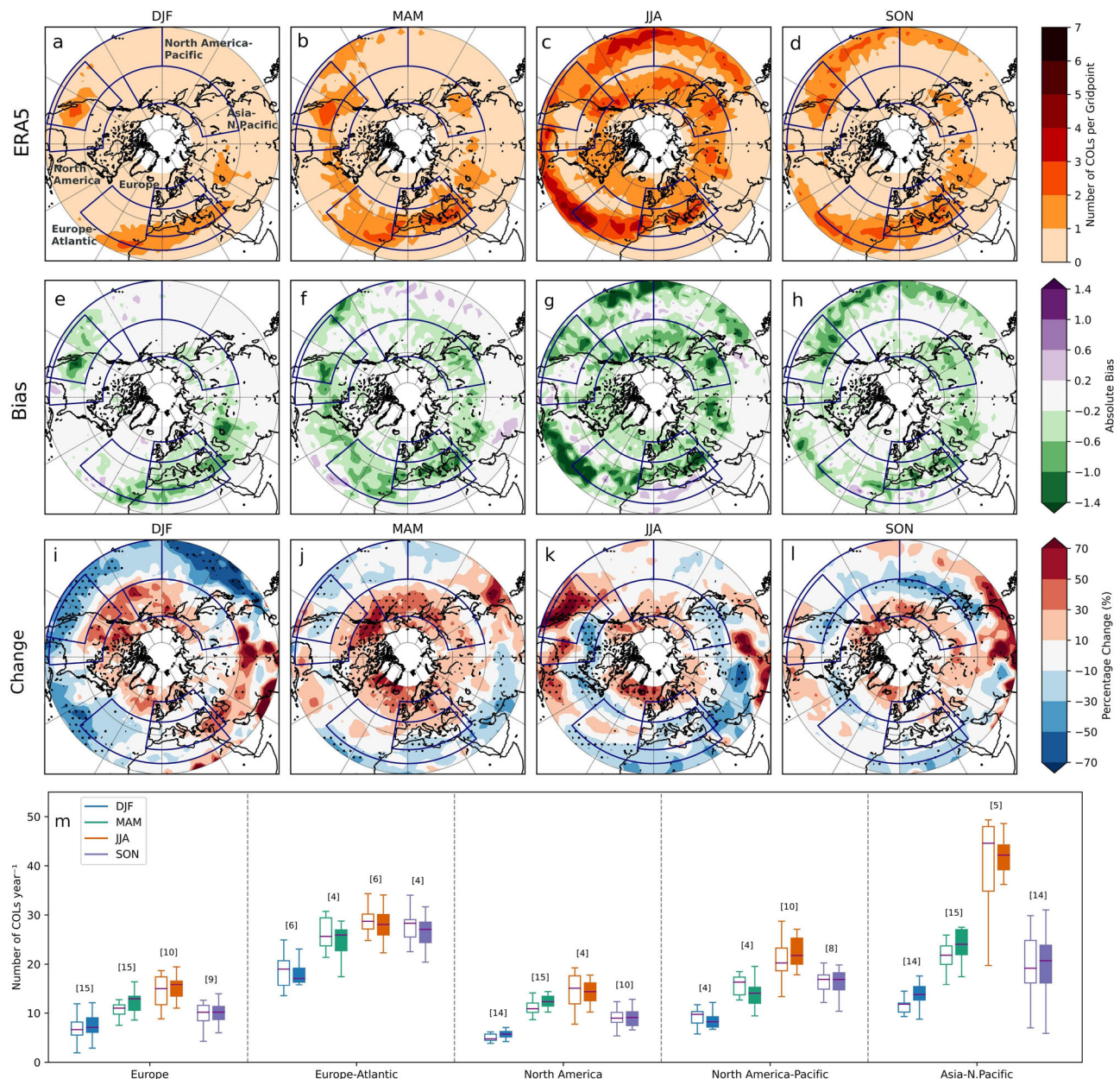
Fig. 1 | Changes in COL frequency. a–d Annual climatology of the spatial distribution of COLs in ERA5 reanalysis (1979–2014). **e–h** The bias in COL frequency in CMIP6 ensemble mean (1979–2014) compared to ERA5 (1979–2014). **i–l** Percentage change in COL frequency in CMIP6 SSP5-8.5 scenario (2071–2100) compared to CMIP6 historical dataset (1950–2014). **m** Absolute number of COLs per year identified within the regional boxes in (**i–l**) for the historical (empty) and SSP5-8.5 (shaded) datasets on a seasonal basis. The center of the box is the median, the edges of the box extend to the 25th–75th percentiles, and the whiskers extend to the 5th–95th percentiles. The number over the boxplot indicates the models projecting an increase in the future. Stippling denotes statistical significance at the 5% level using the bootstrapping method.

max intensity less than $10 \times 10^{-5}\,\mathrm{s}^{-1}$ (low intensity) and COLs with max intensity higher than $10 \times 10^{-5}\,\mathrm{s}^{-1}$ (high intensity).

The distribution of COLs across all four seasons is much more even for short-lasting COLs, as the summer frequency is much higher for long-lasting COLs (Fig. 2e, j). Moreover, short-lasting COLs are further projected to get less frequent in summer over all land regions (20% change in median) (Fig. 2e). On the other hand, long-lasting COLs are critically projected to become more frequent over Europe in spring as well as in summer with 15/18 and 16/18 models indicating a positive change respectively (Fig. 2e). Certain areas over central and northern Europe project a mean rise of up to 70% (Fig. 2g). Long-lasting COLs are also projected to get more frequent in spring over North America and Asia-N. Pacific, with 13/18 and 16/18 showing a positive change.

Low-intensity COLs are most prominent in summer over all regions (Fig. 3e), and their frequency is projected to increase over the oceans substantially with climate change. A median increase in frequency of 15% is projected for Europe-Atlantic and Asia-N. Pacific regions, while a median rise of 20% is projected for North America and North America-Pacific in summer (Fig. 3e). This is owing to an increase in COL frequency along the North American west coast (Fig. 3c). On the other hand, high-intensity COLs are distributed comparatively evenly around the year over all regions, except Asia-N. Pacific (Fig. 3j). Contrary to low-intensity COLs, high-intensity COL frequency is projected to decrease over the oceans in the summer with a median change in frequency of about 25% for Europe-Atlantic and 20% for North America-Pacific and Asia-N.Pacific (Fig. 4f–i). Over the land regions, however, a significant surge in COL frequency is
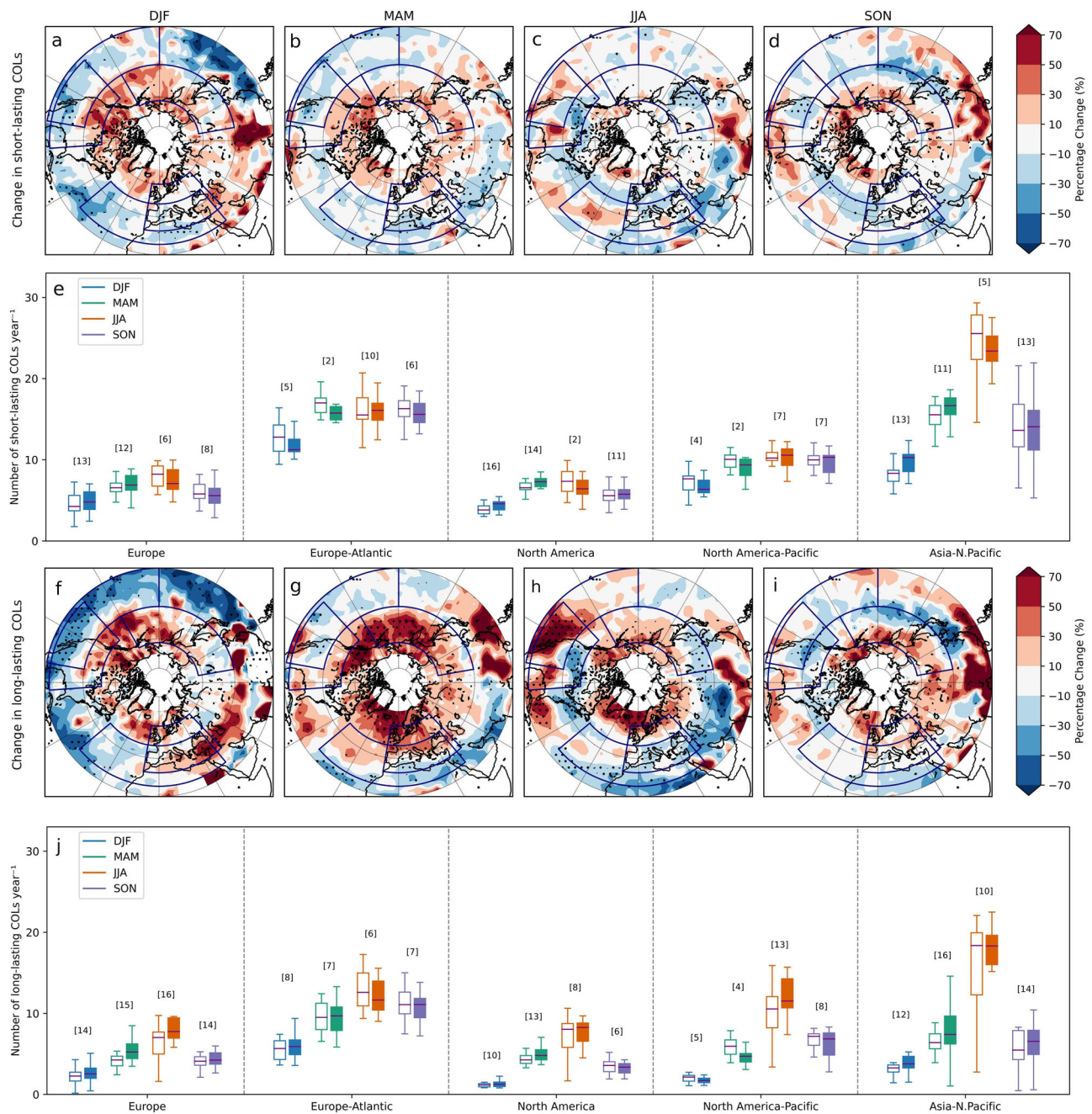
Fig. 2 | Changes in COL frequency based on duration. a–d Percentage change in COL frequency in CMIP6 SSP5-8.5 scenario (2071–2100) compared to CMIP6 historical dataset (1950–2014) for COLs lasting 3 days or less. **e** Absolute number of COLs per year identified within the regional boxes in (**a–d**) for the historical (empty) and SSP5-8.5 (shaded) datasets on a seasonal basis. **f–i** Percentage change in COL frequency in CMIP6 SSP5-8.5 scenario (2071–2100) compared to CMIP6 historical dataset (1950–2014) for COLs lasting over 3 days. **j** Absolute number of COLs per year identified within the regional boxes in (**f–i**) for the historical (empty) and SSP5-8.5 (shaded) datasets on a seasonal basis. The center of the box is the median, the edges of the box extend to the 25th–75th percentiles, and the whiskers extend to the 5th–95th percentiles. The number over the boxplot indicates the models projecting an increase in the future. Stippling denotes statistical significance at the 5% level using the bootstrapping method.

projected in winter, spring, and autumn (Fig. 4f–i). Especially in Europe and Asia-N.Pacific, 17/18 models project an increase with a median surge of 20% in the spring season (Fig. 4j). In North America as well, 15/18 models project an increase in spring with a median increase of 10% (Fig. 4j).

Projected changes in propagation velocity of COLs

COLs are characterized by their quasi-stationary behavior, yet studies have found it hard to predict their centers accurately[37,38]. Some COLs tend to follow a path with larger curvature compared to others. Due to the larger curvature, while the distance covered by the COL may still be large, the overall displacement is relatively small[15]. Consequently, a slow-moving COL with deep convection could lead to persistent rainfall that accumulates over time[27]. Therefore, the propagation velocity of a COL is a relevant characteristic that may determine its impact.

In this section, the velocity changes of short- and long-lasting COLs are studied. Short-lasting COLs tend to propagate much faster than long-lasting COLs (Fig. 4e, j) over all regions. In the summer, the propagation velocity is the slowest for all COLs (Fig. 4e, j). Consistent with the projected changes in zonal wind at 250 hPa[39], COL propagation velocities, in both classes, are
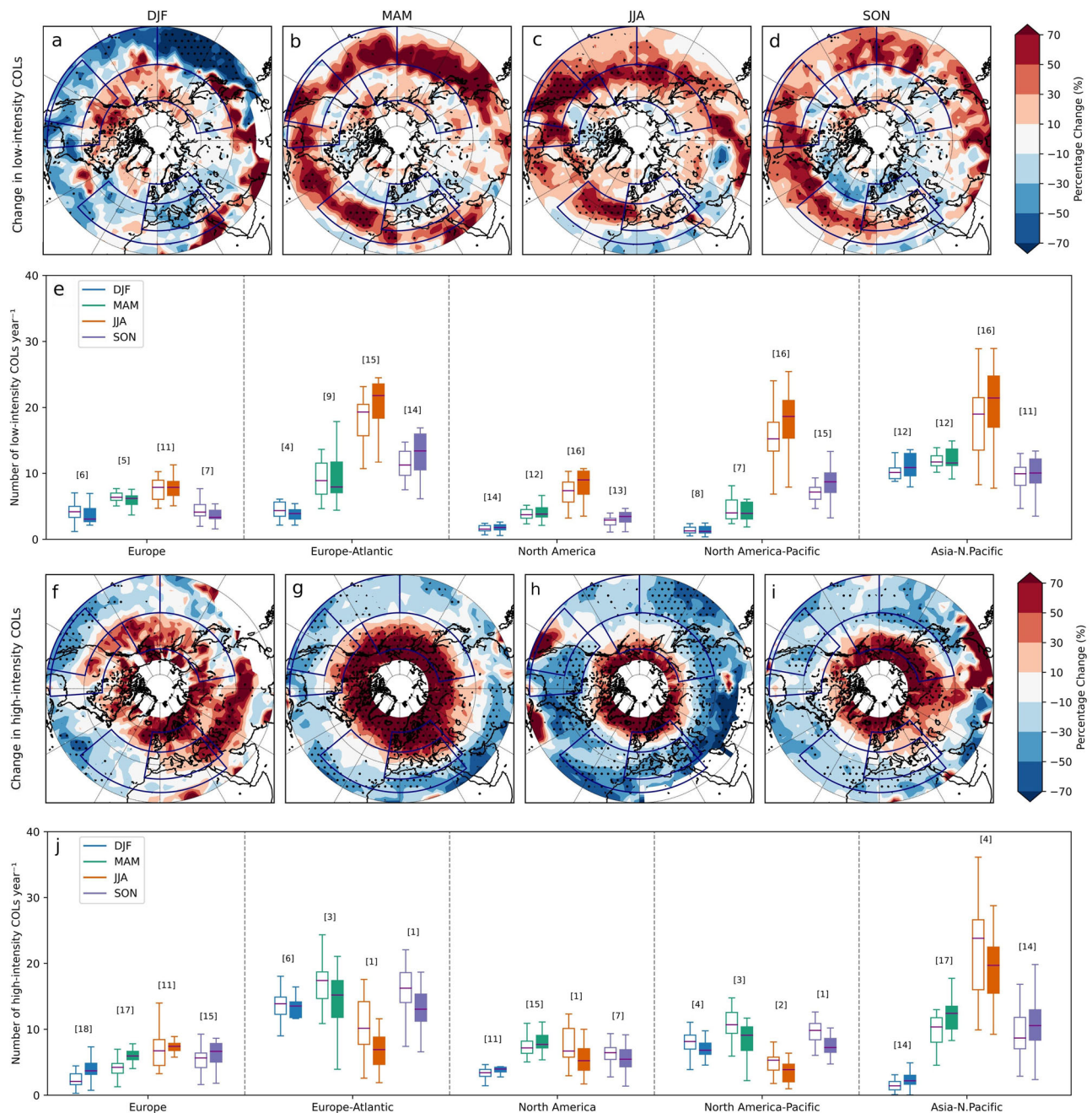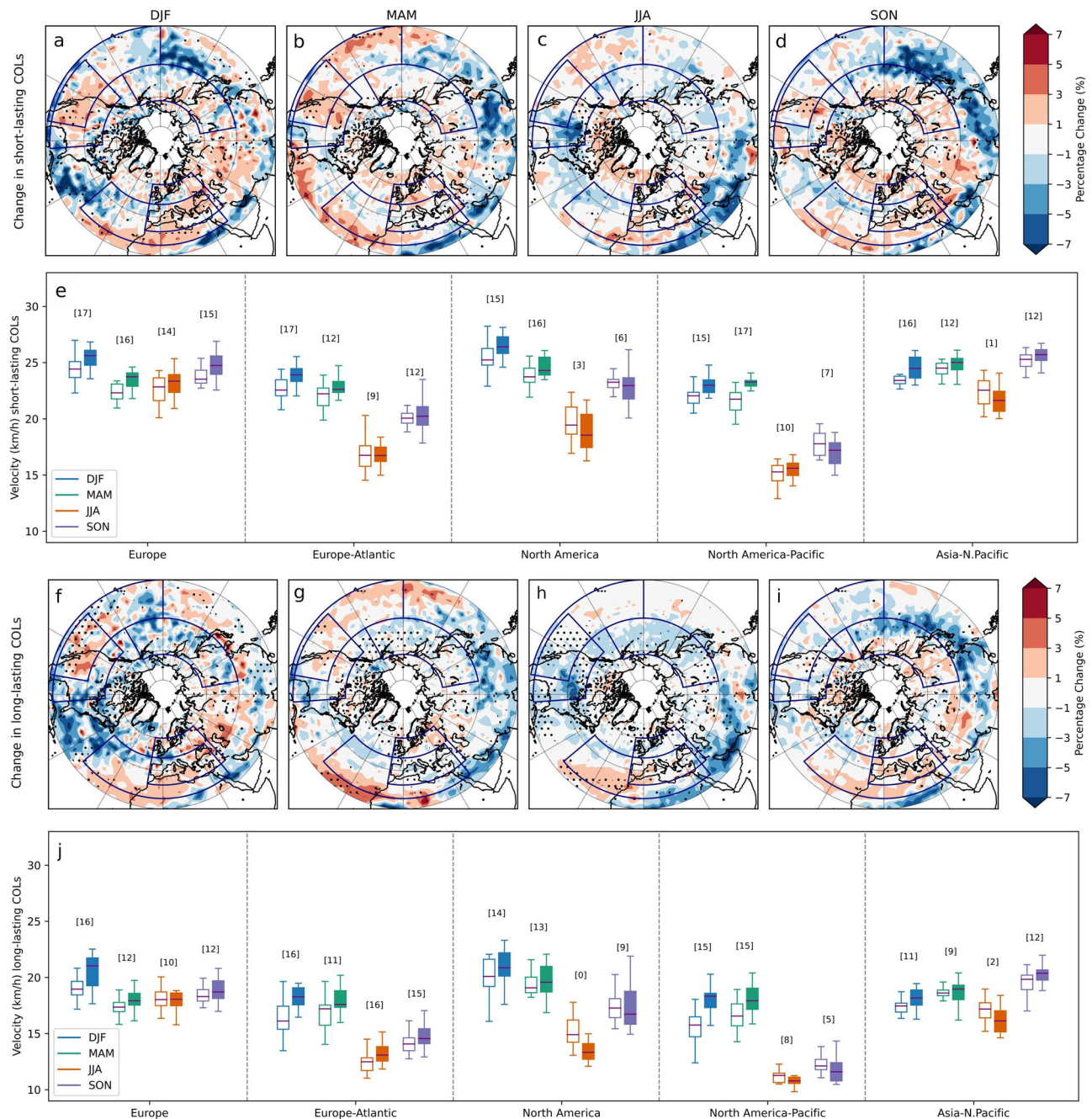
Fig. 3 | Changes in COL frequency based on maximum intensity. a–d Percentage change in COL frequency in CMIP6 SSP5-8.5 scenario (2071–2100) compared to CMIP6 historical dataset (1950–2014) for COLs with max intensity less than or equal to $10 \times 10^{-5}\,\mathrm{s}^{-1}$. **e** Absolute number of COLs per year identified within the regional boxes in (**a–d**) for the historical (empty) and SSP5-8.5 (shaded) datasets on a seasonal basis. **f–i** Percentage change in COL frequency in CMIP6 SSP5-8.5 scenario (2071–2100) compared to CMIP6 historical dataset (1950–2014) for COLs with max intensity more than $10 \times 10^{-5}\,\mathrm{s}^{-1}$. **j** Absolute number of COLs per year identified within the regional boxes in (**f–i**) for the historical (empty) and SSP5-8.5 (shaded) datasets on a seasonal basis. The center of the box is the median, the edges of the box extend to the 25th–75th percentiles, and the whiskers extend to the 5th–95th percentiles. The number over the boxplot indicates the models projecting an increase in the future. Stippling denotes statistical significance at the 5% level using the bootstrapping method.

projected to increase in the future throughout the year over Europe and Europe-Atlantic (Fig. 4e, j). Noticeably, positive changes in winter and spring (Fig. 4a, b, f, g) are much more substantial compared to those in summer and autumn (Fig. 4c, d, h, i). In North America and North America-Pacific as well, winter and spring COLs are projected to propagate faster with climate change (Fig. 4a, b, e, f, g, j). In the summer, however, due to the projected slowing down of the westerly jet over North America and Asia-N.Pacific[39], the COL propagation velocity is also projected to decrease considerably (Fig. 4e, j). Importantly, 18/18 models project a decrease in propagation velocity in summer over North America (Fig. 4j).

Projected changes in the jet stream

Changes in the polar and subtropical jet are linked to Rossby wave-breaking events in the higher troposphere, which in turn may influence the frequency of COLs[40,41]. The eastward propagation of the jet and its increasing zonal flow gives rise to anticyclonic barotropic shear flow and subsequent potential vorticity overturning[22,40]. The COL decay occurs when the jet shifts to the east, ceasing to provide energy to the system. Previous studies have explored this relationship in the context of COL structure and deepening mechanisms, and have also highlighted the uncertainties in establishing a clear-cut relationship[32,42]. Here, the projected changes in the jet stream are

Fig. 4 | Changes in COL propagation velocity based on duration. a–d Absolute change in COL propagation velocity in CMIP6 SSP5-8.5 scenario (2071–2100) compared to CMIP6 historical dataset (1950–2014) for COLs lasting 3 days or less. **e** Absolute propagation velocity of COLs per year identified within the regional boxes in (**a–d**) for the historical (empty) and SSP5-8.5 (shaded) datasets on a seasonal basis. **f–i** Absolute change in COL propagation velocity in CMIP6 SSP5-8.5 scenario (2071–2100) compared to CMIP6 historical dataset (1950–2014) for COLs lasting over 3 days. **j** Absolute propagation velocity of COLs per year identified within the regional boxes in (**f–i**) for the historical (empty) and SSP5-8.5 (shaded) datasets on a seasonal basis. The center of the box is the median, the edges of the box extend to the 25th–75th percentiles, and the whiskers extend to the 5th–95th percentiles. The number over the boxplot indicates the models projecting an increase in the future. Stippling denotes statistical significance at the 5% level using the bootstrapping method.

analysed using the zonal wind field at 250 hPa (Fig. 5) and examined for possible linkages to the changes in the frequency of COLs.

In the northern hemisphere climatology, two major regions of annual COL activity are the Europe-Atlantic and the North America-Pacific regions. In both these regions, COL activity is projected to decrease across all seasons, with the exception of summer in the North America-Pacific region. The increase in summer COL frequency in the North America-Pacific region, specifically around the southwest coast of North America and the Gulf of Mexico, could be related to the projected widespread weakening of the jet northwards over central North America[42]. The weakened zonal flow

is known to favor Rossby Wave Breaking, which may lead to an increase in the frequency of COLs southeastward (downstream) of this region[40]. Similarly, a projected strengthening of the jet over the southeast Pacific in the winter/spring and over the Atlantic Ocean from winter through summer may be responsible for a decrease in COL frequency further southeastward (downstream) of these regions.

As prominent COL regions are projected to become less active in the future, our analysis indicates an increase in COL activity poleward of these regions, thus marking a shift in COL climatology. A weakened zonal flow over Northwest America may be related to the surge in COL frequency
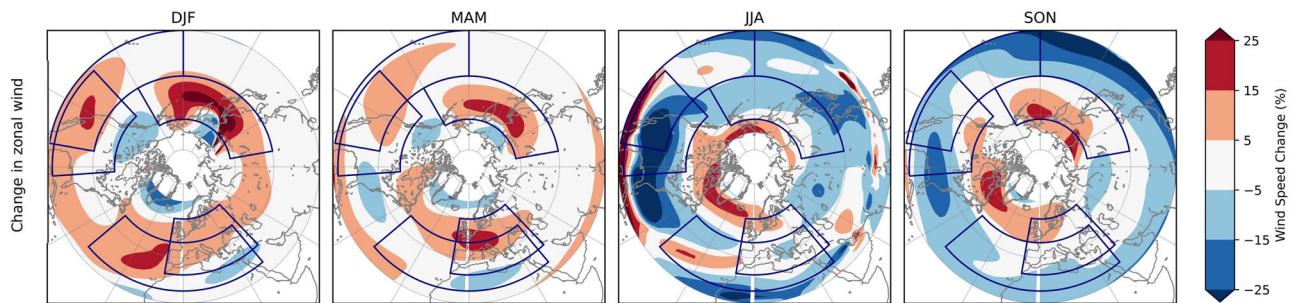
Fig. 5 | Changes in zonal wind. Percentage change in zonal wind in CMIP6 SSP5-8.5 scenario (2071–2100) compared to CMIP6 historical dataset (1950–2014).

further downstream during winter[42]. Over northern Europe in spring, a pronounced dipole pattern is created as a result of a strong polar jet in the south and weak westerlies further up north that enhance cyclonic and anticyclonic vorticity anomalies[43]. The strong jet over Europe is conducive for COL intensification and transport and may explain the widespread increase of COL frequency over Europe in spring.

Discussion

COLs are unique extra-tropical systems, and given their role in causing severe hazards, it is imperative to study how climate change will affect their characteristics in the future. The key results from this study show that the frequency of long-lasting intense COLs is projected to increase over-populated land regions in the Northern Hemisphere. Specifically, COL season over Europe, which is currently confined predominantly to summer, is projected to extend into spring in the future. A similar surge is also projected for North America and Asia-N. Pacific regions, however, unlike Europe, COL frequency is projected to decline here in summer. Importantly, the rise in frequency over these land regions in spring is more pronounced for COLs that are long-lasting and more intense. Such a strong positive change in intense-COL frequency could potentially lead to increased heavy rainfall-related hazards in the future, as accumulated rainfall is highly correlated with COL intensity maxima[24]. Furthermore, the projected changes in COL propagation velocity are also assessed in this study as it is linked to associated rainfall[9,23]. The results suggest that COL propagation velocity will increase in spring, leading to faster-moving COLs, which may partly compensate for the potential increase in hazard caused due to the increase in COL frequency. However, as 80% of all models indicate a surge in severe COL frequency, the potential increase in hazard could still be severe. Conversely, during summer over North America and Asia-N.Pacific, the potential decrease in hazard in the future due to the projected decrease in COL frequency may partly be offset by the projected slowing-down of COLs.

Future changes in the frequency of COLs are interlinked with the changes in jet position, Rossby wave breaking, and atmospheric blocking. However, due to the large uncertainties in the dynamical circulation response to global warming,[44,45] deriving a clear-cut relationship between COLs and its potential proxies is challenging. For instance, atmospheric blocking is often positively linked to COLs[14], and there's a good consensus that atmospheric blocking will decrease with climate change[46]. However, this could be substantially affected by the type of blocking index used to identify the blocking[47]. Despite these uncertainties, projected changes in blocking frequency in certain key regions corroborate the projected changes in COL frequency found in this study. These include the North American west coast, where the blocking frequency is projected to increase in the north and decrease in the south during winter. Also, in the Europe-Atlantic, a projected decrease in blocking frequency in winter may be related to the decline in COL activity. Climatologically speaking, Northern Hemispheric COLs are most prominent in summer due to the general decrease in mid-level westerlies during the warmer months[48]. The analysis of the changes in the zonal flow at 250 hPa suggests a poleward shift in the jet in the future (Fig. 5). This shift can be linked to climate change through different mechanisms such as the poleward expansion of the Hadley cell, the

widening of the tropical belt[49] and the cooling of the stratosphere[50,51]. The rise in COL frequency in spring could be related to an earlier seasonal northward shift in the jet. That being said, there is considerable uncertainty related to the changes in the meandering of the jet[52], which in turn is responsible for the changes in the frequency of atmospheric blocking[46].

In addition to the uncertainties in the projected changes in the atmospheric dynamics, it is imperative to acknowledge that CMIP6 - despite being state-of-the-art tools do not comprehensively represent the observed trends in northern hemispheric blocking frequencies. The biases are most prominent over the European and North Atlantic sectors, including Greenland blocking[46]. Moreover, CMIP6 has been found to underestimate atmospheric circulation changes that are closely linked to COL generation. These include underestimating the frequency and intensity of southerly flow close to western Europe[53] and failing to replicate the strong increasing trend in mid-tropospheric deep depressions in summer over the eastern North Atlantic[54]. Overcoming these limitations in the next generation of models will substantially aid the confidence in the projected trends. Furthermore, the analysis is based on the SSP5-8.5 scenario, representing a high-end, worst-case warming pathway. A similar analysis based on the SSP2-4.5 or SSP1-2.6 scenario focusing on the frequency changes in the middle of the century could also be useful. However, the robustness of the trends observed here underscores their relevance, even if the magnitude of the changes may be moderated under lower-emission scenarios.

The objective of this study is to bring forth future changes in COL frequency based on characteristics that are linked to the associated precipitation. While a number of studies have looked deeper into COL characteristics and the associated precipitation, their analysis is limited to a single event or a specific region[27,55–57]. A comprehensive composite analysis examining COL changes in the future and their implications for precipitation trends, could provide valuable insights. Moreover, the overall impact of a COL is also influenced by its horizontal and vertical structure. Recent studies have linked COL depth and stratospheric intrusion depth[19], and have shown that deeper COLs are associated with more significant surface cyclogenetic forcing[17]. Deeper intrusions lead to more substantial surface pressure decreases and cyclonic circulation, highlighting the importance of the vertical distance of COLs to the surface. The enhanced relative vorticity in the large intrusions also suggests that the vertical height of intrusion could play a role in extreme windstorms[58]. COLs are slow-moving systems and their ability to lead to localized heavy precipitation can also be partially explained through their quasi-stationary behavior. Since the COL is detached from the main westerly flow, it maintains a much slower propagation velocity relative to the jet itself, however, due to the detachment the COL may follow a trajectory that is completely different from the jet[1]. That being said, the parent jet velocity may still influence the propagation velocity of a detached COL. Case in point, the projected changes in the zonal flow[39] corroborate very well with the projected changes in the propagation velocity of COLs (Fig. 4).

Data and methods
Data
In this study, ERA5 is used as the reanalysis dataset, which is the fifth and latest generation of reanalysis from the European Centre for Medium-range

Weather Forecasts (ECMWF)[59]. ERA5 uses the Integrated Forecasting System (IFS) model, specifically Cycle 41r2, and incorporates a 12-h 4DVar data assimilation process. It has a spatial resolution of TL639, which corresponds to ~31 km, and a 1-h temporal resolution. Relative vorticity is extracted from ERA5 at 6-h timesteps for the period 1979–2014 at 250 hPa. The results drawn from ERA5 reanalysis are utilized to evaluate certain results against CMIP6.

For modeled data, 6-h ua wind and va wind data at 250 hPa is used to calculate relative vorticity from 18 Coupled Model Intercomparison Project, Phase 6 (CMIP6) models (Supplementary Table 1). The models are chosen based on the availability of data meeting the aforementioned criteria essential for COL tracking in both historical and future simulations. The historical simulations cover 65 years from 1950 to 2014, while the 30-year future period is taken from 2071 to 2100 for the SSP5-8.5 emission scenario. The selection is a mix of standard CMIP6 models with atmospheric resolutions typically ranging from 250 to 100 km and HighResMIP[60] models with higher resolutions (25–50 km). The CMIP6 models are remapped to a uniform grid to perform the tracking of COLs.

Tracking COLs with TRACK

In this study, a feature-tracking algorithm—TRACK[33–35] is deployed, to detect and track COLs in the NH. The algorithm is used to track COLs in the NH using the relative maxima of the 250 hPa relative vorticity, as it is the level where the highest COL intensities occur[24]. In the future, however, climate change may influence the altitude level at which the highest COL intensities occur (subject to discrete research). The tracking is performed individually on each ensemble model, and the ensemble mean fields are calculated thereafter. The objective tracking of COL features in the relative vorticity field involves three primary stages: spectral filtering, tracking, and four-point wind filtering.

In the first step, data is spectrally truncated to triangular truncation 42 (T42) on a Gaussian grid as relative vorticity is very noisy[61]. Large-scale background is also removed by setting coefficients equal to or less than five for the total wavenumbers to zero, and the Gibbs effect is minimized by applying[62] tapering filter. In the tracking step, firstly, the feature point defined as maxima greater than $1.0 \times 10^{-5} \, \text{s}^{-1}$ is detected as off-grid locations using B-spline interpolation and steepest ascent maximization. Next, an initial collection of tracks is generated based on the identified feature points, employing a nearest-neighbor approach. This initial track set is subsequently refined by minimizing a cost function aimed at enhancing track smoothness while adhering to adaptive constraints concerning displacement and smoothness of the tracks[22]. This is done by minimizing the changes in direction and speed, requiring at least three consecutive frames. Tracks are initialized from feature points, and incomplete tracks are filled with phantom points to ensure consistency in length. The optimization process adjusts points forward and backward in time to maximize smoothness and avoid dependence on feature point order[35]. Cyclonic circulations lasting at least 24 h are retained after this step. Lastly, to identify systems that are cut off from the westerly flow, four-point filtering of the feature points is applied. For this, zonal and meridional wind patterns from four different directions are taken at a radial distance of 5° from the feature point. To filter out open troughs, we look for wind patterns that exhibit a counterclockwise (cyclonic) circulation around the feature point. In particular, the following conditions have to be met: $v_{0°} < 0$ (where $v_{0°}$ is the zonal wind at the offset point of 0° relative to North), $\nu_{90°} > 0$ (with $\nu_{90°}$ being the meridional wind at 90° relative to North), $v_{180°} > 0$, and $\nu_{270°} < 0$. Systems that meet these conditions for a continuous period of at least four frames, which corresponds to 24 h of observation are considered. If the conditions are not met in one frame but are met again in the following four consecutive frames, the track is split and treated as two separate Cut-off Low events, even if the second one may have originated from the first[22].

In this study, COLs are traced using relative vorticity, as it is more efficient in detecting COLs at lower latitudes compared to the other diagnostic (geopotential height)—which is a much smoother field[21]. Despite the preprocessing steps to minimize the latitudinal impact on the

geopotential height field, a lower density of cut-offs is detected with the geopotential height diagnostic. Nevertheless, the intensities obtained from both fields exhibit a comparable distribution, suggesting that the selection of the field does not alter the type of system identified. The results obtained are sensitive to the configuration used in TRACK, which is optimized (keeping a lower feature point detection threshold) to identify a large number of potential COLs. The COLs then get filtered further in the post-tracking step to exclude upper-level troughs. Setting the feature point detection threshold to a higher value may exclude weaker systems. Additionally, setting a very restrictive adaptive constraint may lead to the separation of tracks i.e., an increase in the number of events and a decrease in their lifetime (and vice versa)[35]. The TRACK configuration used in this study is described in detail in ref. 20.

Data availability

The datasets used in this study are available in the public domain for free. CMIP6 data can be accessed publicly through the Earth System Grid Federation at http://esgf.llnl.gov/. The ERA5 reanalysis dataset, produced by the European Centre for Medium-Range Weather Forecasts (ECMWF), is available at https://www.ecmwf.int/en/forecasts/dataset/ecmwf-reanalysis-v5. TRACK software is available for download at https://doi.org/10.5281/zenodo.14441425. The data needed to recreate the figures used in the article can be accessed at https://doi.org/10.5281/zenodo.14618620.

Code availability

The source code for the TRACK software is available at https://gitlab.act.reading.ac.uk/track/track/-/releases. All the analysis and plots are produced using the Python programming language. The code used for the analysis in this study is available upon request from the corresponding author.

References

1. Palmén, E. et al. *Atmospheric Circulation Systems: Their Structure And Physical Interpretation* (Academic Press, 1969).
2. McIntyre, M. & Palmer, T. A note on the general concept of wave breaking for rossby and gravity waves. *Pure Appl. Geophys.* **123**, 964–975 (1985).
3. Maraun, D. et al. A severe landslide event in the alpine foreland under possible future climate and land-use changes. *Commun. Earth Environ.* **3**, 87 (2022).
4. Porcù, F., Carrassi, A., Medaglia, C. M., Prodi, F. & Mugnai, A. A study on cut-off low vertical structure and precipitation in the mediterranean region. *Meteorol. Atmos. Phys.* **96**, 121–140 (2007).
5. Llasat, M.-C., Martín, F. & Barrera, A. From the concept of "kaltlufttropfen"(cold air pool) to the cut-off low. the case of september 1971 in spain as an example of their role in heavy rainfalls. *Meteorol. Atmos. Phys.* **96**, 43–60 (2007).
6. McInnes, K. L., Leslie, L. M. & McBride, J. L. Numerical simulation of cut-off lows on the australian east coast: sensitivity to sea-surface temperature. *Int. J. Climatol.* **12**, 783–795 (1992).
7. Price, J. & Vaughan, G. The potential for stratosphere-troposphere exchange in cut-off-low systems. *Q. J. R. Meteorol. Soc.* **119**, 343–365 (1993).
8. Hoskins, B. J., McIntyre, M. E. & Robertson, A. W. On the use and significance of isentropic potential vorticity maps. *Q. J. R. Meteorol. Soc.* **111**, 877–946 (1985).
9. Kreienkamp, F. et al. Rapid attribution of heavy rainfall events leading to the severe flooding in western europe during july 2021. *World Weather Atribution* (2021).
10. Koks, E., Van Ginkel, K., Van Marle, M. & Lemnitzer, A. Brief communication: critical infrastructure impacts of the 2021 mid-july western european flood event. *Nat. Hazards Earth Syst. Sci. Discuss.* **2021**, 1–11 (2021).

11. Li, D., Bian, J. & Fan, Q. A deep stratospheric intrusion associated with an intense cut-off low event over east asia. *Sci. China Earth Sci.* **58**, 116–128 (2015).

12. Ancellet, G., Beekmann, M. & Papayannis, A. Impact of a cutoff low development on downward transport of ozone in the troposphere. *J. Geophys. Res. Atmos.* **99**, 3451–3468 (1994).

13. Lee, H. et al. Climate change 2023: Synthesis report. contribution of working groups i, ii and iii to the sixth assessment report of the intergovernmental panel on climate change (2023).

14. Nieto, R. et al. Climatological features of cutoff low systems in the northern hemisphere. *J. Clim.* **18**, 3085–3103 (2005).

15. Fuenzalida, H. A., Sánchez, R. & Garreaud, R. D. A climatology of cutoff lows in the southern hemisphere. *J. Geophys. Res. Atmos*. **110** (2005).

16. Appenzeller, C., Davies, H. & Norton, W. Fragmentation of stratospheric intrusions. *J. Geophys. Res. Atmos.* **101**, 1435–1456 (1996).

17. Barnes, M. A., Ndarana, T., Sprenger, M. & Landman, W. A. Stratospheric intrusion depth and its effect on surface cyclogenetic forcing: an idealized potential vorticity (pv) inversion experiment. *Weather Clim. Dyn.* **3**, 1291–1309 (2022).

18. Gan, M. A. & Dal Piva, E. Energetics of a southeastern pacific cut-off low. *Atmos. Sci. Lett.* **14**, 272–280 (2013).

19. Barnes, M. A., Ndarana, T. & Landman, W. A. Cut-off lows in the southern hemisphere and their extension to the surface. *Clim. Dyn.* **56**, 3709–3732 (2021).

20. Pinheiro, H., Hodges, K. I. & Gan, M. A. Sensitivity of identifying cut-off lows in the southern hemisphere using multiple criteria: implications for numbers, seasonality and intensity. *Clim. Dyn.* **53**, 6699–6713 (2019).

21. Pinheiro, H., Hodges, K. I. & Gan, M. A. An intercomparison of subtropical cut-off lows in the southern hemisphere using recent reanalyses: era-interim, ncep-cfrs, merra-2, jra-55, and jra-25. *Clim. Dyn.* **54**, 777–792 (2020).

22. Pinheiro, H. et al. Are cut-off lows simulated better in cmip6 compared to cmip5? *Clim. Dyn.* **59**, 2117–2136 (2022).

23. Mishra, A. N. et al. Climate change amplified the 2009 extreme landslide event in Austria. *Clim. Change* **176**, 1–18 (2023).

24. Pinheiro, H., Gan, M. & Hodges, K. Structure and evolution of intense austral cut-off lows. *Q. J. R. Meteorol. Soc.* **147**, 1–20 (2021).

25. Stephens, G. L. et al. The cloudsat mission and the a-train: a new dimension of space-based observations of clouds and precipitation. *Bull. Am. Meteorol. Soc.* **83**, 1771–1790 (2002).

26. Griffiths, M., Reeder, M. J., Low, D. J. & Vincent, R. A. Observations of a cut-off low over southern australia. *Q. J. R. Meteorol. Soc.* **124**, 1109–1132 (1998).

27. Favre, A., Hewitson, B., Lennard, C., Cerezo-Mota, R. & Tadross, M. Cut-off lows in the South Africa region and their contribution to precipitation. *Clim. Dyn.* **41**, 2331–2351 (2013).

28. Wernli, H. & Sprenger, M. Identification and era-15 climatology of potential vorticity streamers and cutoffs near the extratropical tropopause. *J. Atmos. Sci.* **64**, 1569–1586 (2007).

29. Muñoz, C., Schultz, D. & Vaughan, G. A midlatitude climatology and interannual variability of 200-and 500-hpa cut-off lows. *J. Clim.* **33**, 2201–2222 (2020).

30. Bell, G. D. & Bosart, L. F. A 15-year climatology of northern hemisphere 500 mb closed cyclone and anticyclone centers. *Mon. Weather Rev.* **117**, 2142–2164 (1989).

31. Nieto, R., Sprenger, M., Wernli, H., Trigo, R. & Gimeno, L. Identification and climatology of cut-off lows near the tropopause. *Ann. N. Y. Acad. Sci.* **1146**, 256–290 (2008).

32. Portmann, R., Sprenger, M. & Wernli, H. The three-dimensional life cycles of potential vorticity cutoffs: a global and selected regional climatologies in era-interim (1979–2018). *Weather Clim. Dyn.* **2**, 507–534 (2021).

33. Hodges, K. A general method for tracking analysis and its application to meteorological data. *Mon. Weather Rev.* **122**, 2573–2586 (1994).

34. Hodges, K. Feature tracking on the unit sphere. *Mon. Weather Rev.* **123**, 3458–3465 (1995).

35. Hodges, K. Adaptive constraints for feature tracking. *Mon. Weather Rev.* **127**, 1362–1373 (1999).

36. Hofmann, T. *A Comparison of Tracking Cut-off Lows in the Geopotential and Relative Vorticity Field.* University of Graz Library. 38.82 - Klimatologie. Master thesis (2022).

37. Bozkurt, D., Rondanelli, R., Garreaud, R. & Arriagada, A. Impact of warmer eastern tropical pacific sst on the march 2015 atacama floods. *Mon. Weather Rev.* **144**, 4441–4460 (2016).

38. Muofhe, T. P. et al. Forecasting intense cut-off lows in south africa using the 4.4 km unified model. *Climate* **8**, 129 (2020).

39. Harvey, B., Cook, P., Shaffrey, L. & Schiemann, R. The response of the northern hemisphere storm tracks and jet streams to climate change in the cmip3, cmip5, and cmip6 climate models. *J. Geophys. Res. Atmos.* **125**, e2020JD032701 (2020).

40. Ndarana, T. & Waugh, D. W. The link between cut-off lows and rossby wave breaking in the southern hemisphere. *Q. J. R. Meteorol. Soc.* **136**, 869–885 (2010).

41. Barnes, E. A. & Hartmann, D. L. Detection of rossby wave breaking and its response to shifts of the midlatitude jet with climate change. *J. Geophys. Res. Atmos.* **117** (2012).

42. Pinheiro, H. R., Hodges, K. I. & Gan, M. A. Deepening mechanisms of cut-off lows in the southern hemisphere and the role of jet streams: insights from eddy kinetic energy analysis. *Weather Clim. Dyn.* **5**, 881–894 (2024).

43. Bals-Elsholz, T. M. et al. The wintertime southern hemisphere split jet: structure, variability, and evolution. *J. Clim.* **14**, 4191–4215 (2001).

44. Shepherd, T. G. Atmospheric circulation as a source of uncertainty in climate change projections. *Nat. Geosci.* **7**, 703–708 (2014).

45. Vallis, G. K., Zurita-Gotor, P., Cairns, C. & Kidston, J. Response of the large-scale structure of the atmosphere to global warming. *Q. J. R. Meteorol. Soc.* **141**, 1479–1501 (2015).

46. Davini, P. & d'Andrea, F. From cmip3 to cmip6: Northern hemisphere atmospheric blocking simulation in present and future climate. *J. Clim.* **33**, 10021–10038 (2020).

47. Woollings, T., Hannachi, A., Hoskins, B. & Turner, A. A regime view of the north atlantic oscillation and its response to anthropogenic forcing. *J. Clim.* **23**, 1291–1307 (2010).

48. Kentarchos, A. & Davies, T. A climatology of cut-off lows at 200 hpa in the northern hemisphere, 1990–1994. *Int. J. Climatol.* **18**, 379–390 (1998).

49. Seidel, D. J., Fu, Q., Randel, W. J. & Reichler, T. J. Widening of the tropical belt in a changing climate. *Nat. Geosci.* **1**, 21–24 (2008).

50. Haigh, J. D., Blackburn, M. & Day, R. The response of tropospheric circulation to perturbations in lower-stratospheric temperature. *J. Clim.* **18**, 3672–3685 (2005).

51. Williams, G. Circulation sensitivity to tropopause height. *J. Atmos. Sci.* **63**, 1954–1961 (2006).

52. Dorrington, J., Strommen, K., Fabiano, F. & Molteni, F. Cmip6 models trend toward less persistent european blocking regimes in a warming climate. *Geophys. Res. Lett.* **49**, e2022GL100811 (2022).

53. Vautard, R. et al. Heat extremes in western europe increasing faster than simulated due to atmospheric circulation trends. *Nat. Commun.* **14**, 6803 (2023).

54. d'Andrea, F. et al. Summer deep depressions increase over the eastern north atlantic. *Geophys. Res. Lett.* **51**, e2023GL104435 (2024).

55. Muñoz, C. & Schultz, D. M. Cut-off lows, moisture plumes, and their influence on extreme-precipitation. *J. Appl. Meteorol. Clim.* **500**, 20–0135 (2021).

56. Abba Omar, S. & Abiodun, B. J. Simulating the characteristics of cut-off low rainfall over the western cape using wrf. *Clim. Dyn.* **56**, 1265–1283 (2021).

57. Hu, K., Lu, R. & Wang, D. Seasonal climatology of cut-off lows and associated precipitation patterns over northeast china. *Meteorol. Atmos. Phys.* **106**, 37–48 (2010).

58. Liberato, M. L. The 19 january 2013 windstorm over the north atlantic: large-scale dynamics and impacts on iberia. *Weather Clim. Extrem.* **5**, 16–28 (2014).

59. Hersbach, H. Era5 reanalysis is in production. *ECMWF Newsl.* **147**, 5 (2016).

60. Haarsma, R. J. et al. High resolution model intercomparison project (highresmip v1. 0) for cmip6. *Geosci. Model Dev.* **9**, 4185–4208 (2016).

61. Hoskins, B. J. & Hodges, K. I. New perspectives on the northern hemisphere winter storm tracks. *J. Atmos. Sci.* **59**, 1041–1061 (2002).

62. Sardeshmukh, P. D. & Hoskins, B. I. Spatial smoothing on the sphere. *Mon. weather Rev.* **112**, 2524–2529 (1984).

Acknowledgements

Author contributions

A.N.M. did the preprocessing, tracking and postprocessing of cut-off lows with contributions from K.H. D.M. had the idea for the study and designed the approach. D.M., R.S., G.Z., and A.O. contributed to the analysis and the interpretation of the results. A.N.M. wrote the manuscript, with contributions from D.M., R.S., K.H., G.Z., and A.O.

Competing interests

The authors declare no competing interests.

Additional information

Supplementary information The online version contains supplementary material available at https://doi.org/10.1038/s43247-025-02078-7.

Correspondence and requests for materials should be addressed to Aditya N. Mishra.

Peer review information *Communications Earth & Environment* thanks the anonymous reviewers for their contribution to the peer review of this work. Primary Handling Editors: Joy Monteiro, Heike Langenberg. A peer review file is available

Reprints and permissions information is available at http://www.nature.com/reprints

Publisher's note Springer Nature remains neutral with regard to jurisdictional claims in published maps and institutional affiliations.